

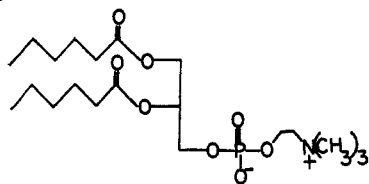
Use of Small-Angle Neutron Scattering To Determine the Structure and Interaction of Dihexanoylphosphatidylcholine Micelles

Tsang-Lang Lin,[†] Sow-Hsin Chen,[†] N. Elise Gabriel,[‡] and Mary F. Roberts*[‡]

Contribution from the Departments of Nuclear Engineering and Chemistry, Massachusetts Institute of Technology, Cambridge, Massachusetts 02139. Received August 21, 1985

Abstract: SANS external and internal contrast variation experiments have been used to determine the structure of dihexanoylphosphatidylcholine micelles. These monodisperse (aggregation number 19 ± 1 from 0.027 to 0.361 M) short-chain lecithin micelles can be well represented by a prolate ellipsoid with two uniform regions. The hydrocarbon chains form a close-packed spheroidal core with a minor axis equal to the fully extended fatty acyl chain (7.8 Å) and a major axis equal to 24.0 Å. Surrounding the hydrocarbon core are the polar head groups, which are distributed in a shell with a thickness of 10 Å in the direction of the minor axis and 6 Å along the major axis. Analysis of the scattering from 1,2-di(hexanoyl-6,6,6-*d*₃)phosphatidylcholine micelles indicates that terminal methyl groups are distributed throughout the hydrocarbon core. At high lecithin concentrations attractive interactions between micelles occur. These can be modeled, and the results suggest that the structure of water around the interface is important in determining effective intermicelle interactions.

Short-chain lecithins have been used extensively to characterize the activity of water-soluble phospholipases.^{1,2} Unlike long-chain lecithins, which form multibilayer vesicles when dispersed in aqueous solution, synthetic lecithins with fatty acyl chain lengths of four to eight carbons form micelles.^{3,4} Dihexanoyl-PC¹ (I)



I

has a critical micelle concentration (cmc) of 14–15 mM^{3,5} and has been studied by a variety of physical techniques.^{4–6} Both NMR and Raman studies have shown that in the micelle the individual dihexanoyl-PC molecules retain many of the conformational features of long-chain lecithins, but they appear very fluid and disordered in the micelle. Dihexanoyl-PC is a poor substrate for phospholipases as a monomer but is rapidly hydrolyzed upon micellization, a phenomenon referred to as “interfacial activation”.⁷ Micellar lecithins are also much better substrates than bilayer structures for these lipolytic enzymes.⁸ The nature of the lecithin aggregate has, therefore, a pronounced effect on enzymatic activity.

To understand these phospholipase kinetics we need to determine micelle structure as well as the motional behavior of the individual lecithin molecules in the micelle. Techniques available for structural determination of macromolecules or assemblies in aqueous solutions include quasi-elastic light scattering,^{9,10} small-angle X-ray scattering,¹¹ and small-angle neutron scattering (SANS).^{12–14} Of these, SANS can provide not only size information^{14–16} but more detailed structural information on individual regions of the aggregate via contrast variation techniques.^{17,18} Changing the contrast between the aggregate particle and the solvent can be achieved by either varying the D₂O/H₂O ratio of the solvent or selectively deuterating the solute molecules. With contrast variation, one can examine different portions of the particles and obtain structural information to about 5–10-Å spatial resolution. SANS has been used successfully to determine the structure of other micelles [for example, lithium dodecyl sulfate¹⁹ and sodium *p*-(1-pentylheptyl)benzenesulfonate²⁰ species]. SANS solvent contrast variation methodology has also been used on phospholipid dispersions in excess water to monitor bilayer

thickness and lateral-phase separation in mixed-phospholipid dispersions.²¹ In this paper we present the results of extensive SANS measurements on dihexanoyl-PC micelles that lead to a detailed structural model for this aggregate and allow development of an interaction model that accounts for the nonideality of high concentrations of micellar solutions.

Materials and Methods

Dihexanoyl-PC was obtained from Calbiochem-Boehringer Corp. 1,2-Perdeuteriohexanoyl-PC and 1,2-di(hexanoyl-6,6,6-*d*₃)-PC were synthesized from glycerophosphorylcholine and the appropriate fatty acid imidazolide as described previously.²² Hexanoic-*d*₁₁ acid and hexa-

- (1) DeHaas, G. H.; Bensen, P. P. M.; Peiterson, W. A.; Van Deenen, L. M. *Biochim. Biophys. Acta* **1971**, *239*, 252.
- (2) Wells, M. A. *Biochemistry* **1974**, *13*, 2248.
- (3) Tausk, R. J. M.; Karmiggelt, J.; Oudshoorn, C.; Overbeek, J. Th. G. *Biophys. Chem.* **1974**, *1*, 175.
- (4) Tausk, R. J. M.; Van Esch, J.; Karmiggelt, J.; Voordouw, G.; Overbeek, J. Th. G. *Biophys. Chem.* **1974**, *1*, 184.
- (5) Burns, R. A., Jr.; Roberts, M. F.; Dluhy, R.; Mendelsohn, R. J. *Am. Chem. Soc.* **1982**, *104*, 430.
- (6) Burns, R. A., Jr.; Stark, R. E.; Vidusek, D. A.; Roberts, M. F. *Biochemistry* **1983**, *22*, 5084.
- (7) Verger, R.; DeHaas, G. H. *Annu. Rev. Biophys. Bioeng.* **1976**, *5*, 77.
- (8) Kensil, C. A.; Dennis, E. A. *J. Biol. Chem.* **1979**, *254*, 5843.
- (9) Chen, S.-H.; Chu, B.; Nossal, R. *Scattering Techniques Applied to Supramolecular and Non-Equilibrium Systems*, NATO ASI Series B73; Plenum: New York, 1981.
- (10) Burns, R. A., Jr.; Donovan, J. M.; Roberts, M. F. *Biochemistry* **1983**, *22*, 964.
- (11) Laggner, P.; Muller, K. W. *Q. Rev. Biophys.* **1978**, *11*, 3711.
- (12) Schneider, D. K.; Schoenborn, B. P. *Neutrons in Biology*; Schoenborn, B. P., Ed.; Plenum: New York, 1984; p 119.
- (13) Engelman, D. M.; Moore, P. B. *Annu. Rev. Biophys. Bioeng.* **1975**, *4*, 219.
- (14) Chen, S.-H.; Lin, T.-L. In *Methods of Experimental Physics—Neutron Scattering*; Sköld, K., Price, D. L., Eds.; Academic: New York, 1986; Vol. 2.
- (15) Jacrot, B. *Rep. Prog. Phys.* **1976**, *39*, 911.
- (16) Jacrot, B.; Zaccai, G. *Biopolymers* **1981**, *20*, 2413.
- (17) Stuhmann, H. B. *J. Appl. Crystallogr.* **1974**, *7*, 173.
- (18) Kneale, G. G.; Baldwin, J. P.; Bradbury, E. M. *Q. Rev. Biophys.* **1977**, *10*, 485.
- (19) Bendedouch, D.; Chen, S.-H.; Koehler, W. C. *J. Phys. Chem.* **1983**, *87*, 153.
- (20) Magid, L. J.; Triolo, R.; Johnson, J. S., Jr.; Koehler, W. C. *J. Phys. Chem.* **1982**, *86*, 164.
- (21) Knoll, W.; Haas, J.; Stuhmann, H. B.; Fuldner, H.-H.; Vogel, H.; Sackmann, E. *J. Appl. Crystallogr.* **1981**, *14*, 191.
- (22) Boss, W. F.; Kelley, C. J.; Landsberger, F. R. *Anal. Biochem.* **1975**, *64*, 289.

[†] Department of Nuclear Engineering.

[‡] Department of Chemistry.

noic-6,6,6- d_3 acid were obtained from Merck Sharp and Dohme Isotopes. Lipid purity was monitored by thin-layer chromatography as described previously.²³ Phosphate analyses were done on each sample before and after SANS runs to determine the lecithin concentration.

Most of the SANS measurements of this study were performed with the biology small-angle neutron-scattering spectrometer¹² located at the H9B beam line in the high-flux beam reactor (HFBR) of Brookhaven National Laboratory. Cold neutrons were derived from a solid-hydrogen cold-neutron source located in the beam thimble of H9B beam line. Polychromatic cold neutrons were filtered through cold polycrystalline Be and then passed through a multilayered monochromator to obtain a well-defined primary beam of wavelength $\lambda = 4.75 \text{ \AA}$ with a spread $\Delta\lambda/\lambda = 10\%$. Samples were placed in disk-shaped quartz cells. The path length of the sample varied from 1 to 4 mm. Choice of the path length was based on a criterion that the transmission factor should be higher than 0.8. Under this condition multiple scattering effects are negligible. Typically, 1-mm path-length cells were used for solution concentrations higher than 0.05 M. Initially, a two-dimensional neutron detector of size 17 cm \times 17 cm was used. Later data acquisition used a 50 cm \times 50 cm detector. The sample to detector distance was set at 1.4 m with the entrance circular pinhole (12-mm diameter) at a distance of 1.36 m from the sample pinhole (6-mm diameter). When the neutron beam axis is moved from the center to the corner of the detector, a wide range of Q (the magnitude of the scattering vector) from 0.02 to 0.25 \AA^{-1} is covered. This is a suitable Q range for isotropic solutions containing particles around 25 \AA . The measured scattering intensities are then circularly averaged to give the neutron scattering intensities vs. Q . For samples with D_2O as the solvent, 1–2 h are required to get good signal to noise ratio for each measurement. Those samples containing H_2O require a much longer time to get good counting statistics.

A 1-mm water sample was used as a standard scatterer to calibrate the detector efficiency. The measured scattering intensities were corrected for the detector background, the scattering from the quartz cell, and the detector sensitivity¹⁴ and finally put into an absolute unit of the differential scattering cross section per unit sample volume by using the transmission factor of the 1-mm water (H_2O) sample.¹⁶

For contrast variation measurements, samples containing 50 mM dihexanoyl-PC were used. At this concentration the interactions between micelles were found to be weak (vide infra). The external contrast variations were made by varying the volume ratio of D_2O to H_2O , designated α , from 1 to 0.776, 0.576, 0.369, and 0. Values of α were accurately determined from the neutron transmission factors using $\alpha = 1$ and $\alpha = 0$ samples as references. The internal contrast variations were made by using samples containing mixtures of perdeuterated fatty acyl chain lecithin and proteodihexanoyl-PC. The molar ratio, β , of the deuterated and the proteodihexanoyl-PC varied from 0 to 0.2, 0.4, 0.6, 0.8, and 1.0. To study the dependence of micellar interactions on concentration, a series of measurements were made with solutions containing 0.027, 0.050, 0.099, 0.191, and 0.361 M dihexanoyl-PC in D_2O .

Measurements comparing di(hexanoyl-6,6,6- d_3)-PC with its proteo counterpart were performed with the 30-M SANS instrument at the National Center for Small-Angle Scattering Research located at the high-flux isotope reactor (HFIR) of Oak Ridge National Laboratory. Both lecithin samples were 0.05 M in D_2O .

Results and Discussion

External Contrast Variation. For a liquid sample of volume V consisting of N micelles dispersed in a solvent the neutron scattering cross section per unit volume at a scattering vector \vec{Q} is given by¹⁴

$$I(Q) = \frac{1}{V} \sum_{j=1}^N |F_j(\vec{Q})|^2 S'(Q) \quad (1)$$

where

$$F_j(\vec{Q}) = \int [\rho_j(\vec{r}) - \rho_s] e^{i\vec{Q}\cdot\vec{r}} d^3r \quad (2)$$

Here $F_j(\vec{Q})$ is the form factor of the j th micelle. $\rho_j(\vec{r})$ is the coherent neutron scattering length density (csld) of the micelle and ρ_s the csld of the solvent, which is considered uniform in space. The integration is over the volume occupied by the j th micelle. The term $S'(Q)$ represents the size and orientation weighted interparticle structure factor, which will be discussed when we deal with high lecithin concentrations. From eq 2 one sees that the scattering intensities depend on the difference (contrast)

between the csld of the micelle and the solvent. In the dilute limit when interactions between micelles can be neglected, $S'(Q)$ will reduce to unity, and from eq 1 and 2

$$I(Q) = \frac{1}{V} \sum_{j=1}^N |[\rho_j(\vec{r}) - \rho_s] e^{i\vec{Q}\cdot\vec{r}} d^3r|^2 \quad (3)$$

The quantity $\rho_j(\vec{r})$ contains the information about the structure of the j th micelle. In general one cannot obtain $\rho_j(\vec{r})$ from $I(Q)$ directly by taking the inverse Fourier transform of the square root of $I(Q)$. This is only possible for a collection of monodispersed spherical particles having symmetric structure, i.e., $\rho_j(\vec{r}) = \rho_j(r)$, where the scattering intensities have been accurately measured up to a very large Q region in order to avoid error due to truncation of the $I(Q)$ in the Fourier transform.

A practical approach to obtain structure is to use contrast variation methods. It is more convenient to consider the right-hand side of eq 3 as comprised of a Q -independent amplitude term I_0 multiplied by a normalized structure factor $P(Q)$:

$$I(Q) = I_0 P(Q) \quad (4)$$

where

$$I_0 = \frac{1}{V} \sum_{j=1}^N \int |\rho_j(\vec{r}) - \rho_s|^2 d^3r \quad (5)$$

$$P(Q) = \frac{\sum_{j=1}^N \int [\rho_j(\vec{r}) - \rho_s] e^{i\vec{Q}\cdot\vec{r}} d^3r}{\sum_{j=1}^N \int |\rho_j(\vec{r}) - \rho_s|^2 d^3r} \quad (6)$$

and $P(Q)$ is equal to 1 at $Q = 0$. The amplitude term I_0 depends not on the micellar shape but on the aggregation number. Upon integrating eq 5 one obtains

$$I_0 = \frac{1}{V} \sum_{j=1}^N [n_j (b_m - \rho_s V_m)]^2 \quad (7)$$

Here n_j is the number of dihexanoyl-PC molecules in the j th micelle, b_m is the sum of the coherent neutron scattering lengths of the molecule that can be computed from the known chemical formula of dihexanoyl-PC by using tabulated neutron scattering lengths,²⁵ and V_m is the volume occupied by each monomer in the micellar aggregate.

It was concluded by Tausk et al.⁴ from an extensive light scattering experiment that dihexanoyl-PC micelles have a rather narrow weight distribution. Our neutron scattering spectra of dihexanoyl-PC also exhibit low polydispersity as compared to that of other systems studied by SANS.²⁶ Since the dihexanoyl-PC micelles either are monodispersed or have low polydispersity, the system can be approximated as monodispersed micelles with a mean aggregation number \bar{n} . Equation 7 then becomes

$$I_0 = (C - C_{cmc}) \bar{n} (b_m - \rho_s V_m)^2 \quad (8)$$

Here, C and C_{cmc} each are the concentrations of the short-chain lecithin and its critical micellar concentration, respectively, in units of number of lecithin molecules per unit volume. In the small- Q region for particles having a center of symmetry, eq 4 can be written in the Guinier approximation²⁷ as

$$I(Q) = I_0 \exp(-Q^2 R_g^2 / 3) \quad (9)$$

where R_g is the radius of gyration of the micelle defined by

$$R_g = \left[\frac{\int r^2 [\rho_j(\vec{r}) - \rho_s] d^3r}{\int [\rho_j(\vec{r}) - \rho_s] d^3r} \right]^{1/2} \quad (10)$$

In general, the value of R_g depends on the contrast $\rho_j(\vec{r}) - \rho_s$. The

(23) Burns, R. A., Jr.; Roberts, M. F. *Biochemistry* 1980, 19, 3100.

(24) Schelten, J.; Schmatz, W. *J. Appl. Crystallogr.* 1980, 13, 385.

(25) Bacon, G. E. *Neutron Diffraction*, 3rd. ed.; (1980) Oxford: New York, 1980.

(26) Kotlarchyk, M.; Chen, S.-H.; Huang, J. S. *J. Phys. Chem.* 1983, 86, 3273.

(27) Guinier, A.; Fournet, G. *Small Angle Scattering of X-Rays*; Wiley: New York, 1955.

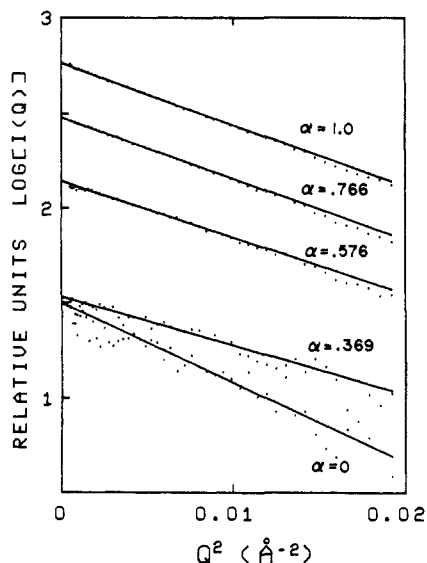


Figure 1. Guinier plots of the intensity distribution from the external contrast variation expts. of dihexanoyl-PC (0.050 ± 0.010 M). The scattering intensities change with α , the volume fraction of D_2O in the solvent. From the straight lines the scattering amplitudes and the radii of gyration are determined.

external contrast variation involves using different mixtures of H_2O with D_2O in order to change ρ_s . Thus, a Guinier plot of $\ln [I(Q)]$ vs. Q^2 will be a straight line in the small- Q region with a slope of $-R_g^2/3$. Figure 1 shows the Guinier plots for the external contrast variation series. The experimental data are fit by straight lines for $Q^2 = 0.0025$ – 0.01 \AA^{-2} to determine I_0 and R_g . Both I_0 and R_g are functions of the fractional deuteration of the solvent, α , and the csld's of H_2O and D_2O :

$$\rho_s(\alpha) = \rho_{H_2O}(1 - \alpha) + \rho_{D_2O}\alpha \quad (11)$$

At $\alpha = 0.369$ and $\alpha = 0$, the experimental data are scattered because the contrast is low and the incoherent background due to H_2O is large. The radius of gyration was found to decrease gradually from 14.9 ± 0.2 to $13.3 \pm 0.7 \text{ \AA}$ when the solvent changed from D_2O to a mixture of 36.9% D_2O and 73.1% H_2O . This is an indication that the head groups of dihexanoyl-PC molecules on average lie at a further distance from the center of the micelle than do the hydrocarbon tails. By estimation of the steric volume of the head group and the tails, the head group is found to have a mean csld lying between ρ_{D_2O} and ρ_{H_2O} while the protonated tails have a mean csld close to ρ_{H_2O} . Thus, when the volume fraction of H_2O in the solvent increases from zero, the contrast between the head groups and the solvent gradually decreases and the weights that determine R_g gradually shift to the region of hydrocarbon tails. Since R_g initially decreases as α is increased, the tails on average must be at a smaller distance from the center of the micelle.

At $\alpha = 0$, i.e., for a pure H_2O solvent, the contrast between the tails and the solvent is almost zero, and thus scattering of neutrons comes largely from the head-group region. In other words neutrons see only the head groups when the csld of the tails is nearly matched by the csld of the solvent. Indeed for this case a larger value of R_g (17.0 \AA) is obtained.

The scattering amplitudes extracted from the Guinier plots can be normalized to a concentration at 50 mM and plotted as $\pm(I_0)^{1/2}$ vs. $(1 - \alpha)$ as shown in Figure 2. Combining eq 8 with eq 11, one obtains

$$\pm(I_0)^{1/2} = [(C - C_{cmc})\bar{n}]^{1/2} [\rho_{D_2O} - (1 - \alpha)(\rho_{D_2O} - \rho_{H_2O})] V_m - b_m \quad (12)$$

The square root of I_0 is therefore a linear function of $(1 - \alpha)$, and \bar{n} and V_m can be determined: for dihexanoyl-PC, $\bar{n} = 19 \pm 1$ and $V_m = 670 \pm 100 \text{ \AA}^3$. The scattering amplitude vanishes at $\alpha = 17.7 \pm 1.5\%$, where the mean csld of the micelle is matched to the solvent.

diC₆ LECITHIN
EXTERNAL CONTRAST VARIATION

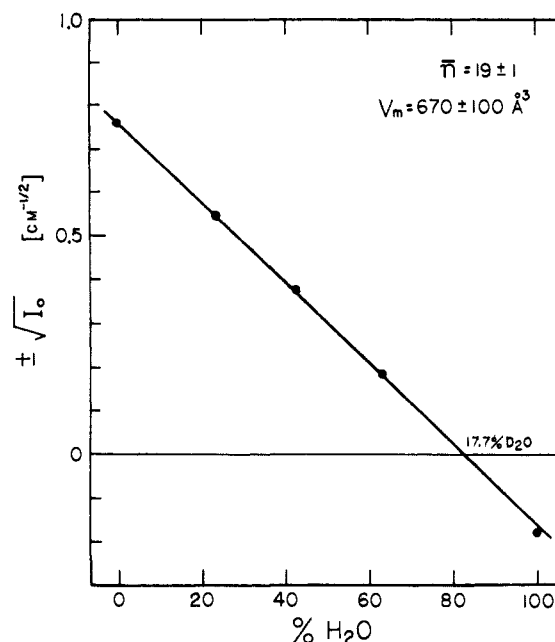


Figure 2. Results of external contrast variation: The zero-intensity intercept occurs at 17.7 vol % D_2O in the solvent; the slope of the straight line gives the aggregation number and the zero intercept the volume occupied by a dihexanoyl-PC molecule in the micellar state.

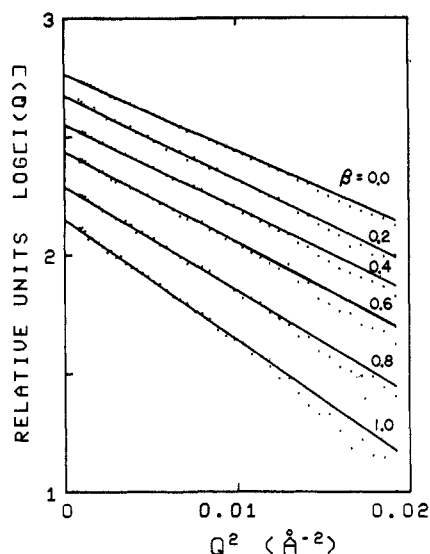


Figure 3. Guinier plots of the intensity distribution from the internal contrast variation experiments with dihexanoyl-PC (0.050 ± 0.010 M). The molar fraction of fatty acyl perdeuterated dihexanoyl-PC is denoted as β ; the radii of gyration increase with increasing β .

Internal Contrast Variation. Instead of varying α , the internal contrast variation method changes b_m by mixing proteo-dihexanoyl-PC with chain-perdeuterated dihexanoyl-PC. Figure 3 shows the Guinier plots for the internal contrast variation measurements. The experimental data presented as $\ln I(Q)$ vs. Q^2 are well fit in the small- Q region. The radius of gyration is found to increase monotonically from 14.9 ± 0.2 to $18.7 \pm 0.3 \text{ \AA}$ as the protonated molecules are gradually replaced by the chain-perdeuterated dihexanoyl-PC. Since deuteration decreases the mean contrast between the tails and the D_2O solvent, the weight that determines the R_g is shifted gradually to the head-group region. Analogous to eq 12, one has in this case

$$\pm(I_0)^{1/2} = [(C - C_{cmc})\bar{n}]^{1/2} [\rho_{D_2O} V_m - [\beta b_m^D + (1 - \beta)b_m^H]] \quad (13)$$

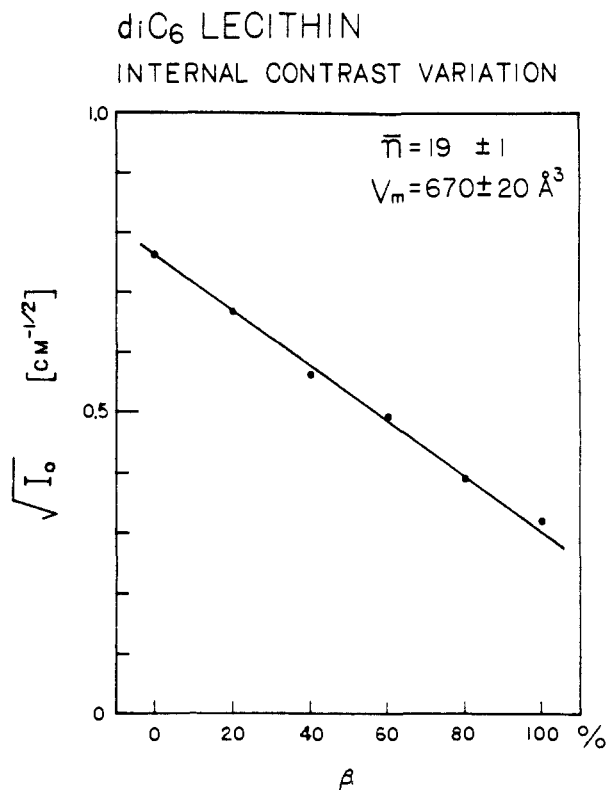


Figure 4. Results of internal contrast variation: The data represent corrected scattering amplitudes (i.e., all points normalized to 0.05 M dihexanoyl-PC). The aggregation number and the volume occupied by a dihexanoyl-PC molecule in the micellar state are determined as in Figure 2.

Here, b_m^D and b_m^H are equal to 273.37×10^{-5} and 44.24×10^{-5} Å for the chain-perdeuterated and the protonated dihexanoyl-PC molecules. The plot of $\pm(I_0)^{1/2}$, normalized at 50 mM, vs. β gives a straight line according to eq 13 (Figure 4). The aggregation number is found to be 19 ± 1 , and $V_m = 670 \pm 20 \text{ \AA}^3$. These values are within the experimental error of those determined by external contrast variation. It should be noted that V_m is determined with a higher accuracy by the internal contrast variation. From density measurements Tausk et al.⁴ have calculated the molar volume of dihexanoyl-PC in micelles to be $410.3 \text{ cm}^3/\text{mol}$, which is equivalent to $681 \text{ \AA}^3/\text{molecule}$, in good agreement with our results from the contrast variation measurements. Though an aggregation number of about 35 has been reported from other techniques,⁴ the SANS method is more direct and therefore the result is more reliable and accurate.

Structure of Dihexanoyl-PC Micelles. Since the radius of gyration varies when the csld of the solvent is changed, the micelles cannot have a uniform structure. A reasonable model is to consider the micelle as consisting of two regions: The inner region contains the fatty acyl chains, and the outer region contains the phosphodiester head group and the glycerol backbone. In the simplest model one can assume that the acyl chains and the head groups are distributed in each region in a uniform way, and thus one can assign constant R_g 's to each region. (The uniformity required is on a scale larger than the spacing between two neighboring atoms since SANS does not have a spatial resolution down to the atomic dimension.) If all the R_g 's from the contrast variation measurements can be explained by this two-region model, it is a valid description of the dihexanoyl-PC micelle. For such a model eq 10 can be rewritten as

$$R_g^2 = \frac{R_{g,1}^2 W_1 + R_{g,2}^2 W_2}{W_1 + W_2} \quad (14)$$

where the subscripts 1 and 2 represent regions 1 and 2, which correspond to the region containing the tails (acyl chains) and

Table I. Comparison of the Measured with the Computed Radii of Gyration^a

Internal Contrast Variation ($\alpha = 1$)				
β	$W_1/(W_1 + W_2)$	$W_2/(W_1 + W_2)$	$R_g, \text{ \AA}$	
			measd	computed
0	0.581	0.419	14.9 ± 0.2	14.92
0.2	0.524	0.476	15.7 ± 0.2	15.30
0.4	0.448	0.552	15.7 ± 0.2	15.79
0.6	0.344	0.656	16.3 ± 0.2	16.43
0.8	0.023	0.977	17.4 ± 0.2	17.33
1.0	-0.053	1.053	18.7 ± 0.3	18.68
External Contrast Variation ($\beta = 0$)				
α	$W_1/(W_1 + W_2)$	$W_2/(W_1 + W_2)$	$R_g, \text{ \AA}$	
			measd	computed
1.0	0.581	0.419	14.9 ± 0.2	14.92
0.766	0.620	0.380	14.9 ± 0.2	14.66
0.576	0.685	0.315	14.4 ± 0.2	14.22
0.369	0.902	0.098	13.3 ± 0.7	12.60
0.0	0.028	0.972	17.0 ± 1.5	18.25

^aKey: α , the fraction of D₂O in the solvent; β , the fraction of the chain-perdeuterated dihexanoyl-PC.

the region containing the head groups, respectively, and the weighting factors are given by

$$W_1(\alpha, \beta) = \int [\rho_{\text{tail}}(\beta) - \rho_s(\alpha)] d^3r \quad (15)$$

$$= \bar{n} [b_{\text{tail}}(\beta) - \rho_s(\alpha) V_{\text{tail}}] \quad (16)$$

$$W_2(\alpha, \beta) = \int [\rho_{\text{head}} - \rho_s(\alpha)] d^3r \quad (17)$$

$$= \bar{n} [b_{\text{head}} - \rho_s(\alpha) V_{\text{head}}] \quad (18)$$

The values of V_{tail} , which is the space occupied by the two fatty acyl chains of a dihexanoyl-PC molecule, can be estimated from the empirical rules of Tanford:²⁸

$$V_{\text{tail}} = 2(27.4 + 26.9N_c) \text{ \AA}^3 \quad (19)$$

With $N_c = 5$, V_{tail} is equal to 323.8 \AA^3 . The space occupied by each head group is 346.2 \AA^3 (obtained by subtracting the V_{tail} from $V_m = 670 \text{ \AA}^3$). The numerical values of b_{head} and $b_{\text{tail}}(\beta)$ are given by

$$b_{\text{head}} = 60.06 \times 10^{-5} \text{ \AA} \quad (20)$$

$$b_{\text{tail}}(\beta) = \beta(213.31 \times 10^{-5} \text{ \AA}) + (1 - \beta)(-15.82 \times 10^{-5} \text{ \AA}) \quad (21)$$

Having these values, one may compute W_1 and W_2 as functions of α and β according to eq 16 and 18. From the various measured R_g 's we can then determine, uniquely, $R_{g,1} = 11.8 \pm 0.2 \text{ \AA}$ and $R_{g,2} = 18.4 \pm 0.3 \text{ \AA}$. All the measured R_g 's can be predicted with a reasonable accuracy by this two-region model as shown in Table I.

The next step is to construct a model for the shape and structure of the two regions. The model should, first, have the right $R_{g,1}$ and $R_{g,2}$ and, second, should be able to predict $I(Q)$ not just in the small- Q region but also in the whole measured Q region. The values of $R_{g,1}$ and $R_{g,2}$ were determined without involving any prior assumption of the shape of each region. If the hydrocarbon chains form a spherical region having a radius of gyration of 11.8 \AA , the radius of the sphere will be 15.2 \AA . This value is too large for fatty acyl chains with a length of only 7.83 \AA (computed from $l = 1.5 + 1.265N_c \text{ \AA}^{28}$). The structure must deviate from a sphere, and an acceptable model of this inner region would probably be a spheroid having a minor axis b equal to the fully stretched chain length, 7.83 \AA ,⁴ and a major axis $a = 23.95 \pm 0.5 \text{ \AA}$, which is determined by requiring

$$R_{g,1}^2 = \frac{1}{5}(a^2 + 2b^2) \quad (22)$$

The volume of this spheroid, $\frac{4}{3}\pi ab^2$, with these values is re-

(28) Tanford, C. *The Hydrophobic Effect*, 2nd ed.; Wiley: New York, 1980.

markedly close to the total steric volume of the chains using $\bar{n} = 19$ and $V_{\text{tail}} = 323.8 \text{ \AA}^3$ (determined by SANS). Even considering the uncertainties of the value a in calculating the volume, we can still safely conclude that the fatty acyl chains form a compact core and there are no water molecules penetrating into the core. Similar conclusions, i.e., a sharp water-hydrocarbon boundary, have also been made for sodium dodecyl sulfate micelles [by examining the asymptotic behavior of $I(Q)$ in the large- Q region²⁹] and for lithium dodecyl sulfate micelles (using the core volume determined from SANS contrast variation method¹⁹). Other geometries for the dihexanoyl-PC micelle are less likely. A spherocylindrical shape, having a radius of 7.83 Å and a height of 25.4 Å for the cylinder part, would give $R_{g,1} = 11.8 \text{ \AA}$, but the volume is 12% larger than the close-pack volume of the tails in a micelle. In this case one would have to postulate that there are some cavities on the surface of the core region and the shape is somewhere between a spheroid and a spherocylinder. To distinguish between such subtle differences in the shape and structure, one would have to consider the detailed conformations and packing constraints using a thermodynamic theory. For our purpose here we propose to adopt the spheroid geometry for the core region.

As for the structure of region 2, the polar head group, it is clear that the head groups must form a shell surrounding the hydrocarbon core. We assume that the outer surface of the shell also has the shape of a spheroid. The shape of the shell is characterized by two parameters, t_a and t_b , which are the thicknesses in the directions of the major and the minor axes of the core, respectively. The radius of gyration of the shell is related to t_a and t_b by

$$R_{g,2}^2 = \frac{[(a+t_a)^2 + 2(b+t_b)^2](a+t_a) \times (b+t_b)^2 - (a^2 + 2b^2)ab^2}{5[(a+t_a)(b+t_b)^2 - ab^2]} \quad (23)$$

If $t_a = t_b$, the thickness is equal to 7.88 Å from eq 23 alone. But in order to fit $I(Q)$ in the whole Q range measured and also to satisfy eq 23, the best values are $t_a = 6 \text{ \AA}$ and $t_b = 10 \text{ \AA}$. In this shell region 80.5% of the volume is occupied by the solvent and 19.5% by the head groups. On average, head groups are modeled as uniformly distributed in this shell region. The fully stretched length of the head group (glycerol backbone and phosphocholine) is estimated to be about 14 Å.⁴ Since the shell thicknesses are smaller than the fully stretched length of the head group, the orientation of the phosphocholine is more likely to be perpendicular to the glycerol backbone and parallel to the surface of the hydrocarbon core with orientations similar to that observed in bilayers.^{30,31}

To compare the experimental data with the model, we must calculate the normalized micellar structure factor $P(Q)$ from the proposed model: a spheroid core plus a shell. $P(Q)$ can be computed from the following equation, which is derived from eq 6 by replacing the summation by the integration over orientations of the micelle:

$$P(Q) = \int_0^1 \left[\frac{W_1 - W_2 \frac{V_1}{V_2}}{W_1 + W_2} 3j_1(u_1) + \frac{W_2 + W_2 \frac{V_1}{V_2}}{W_1 + W_2} 3j_1(u_2) \right]^2 d\mu \quad (24)$$

where

$$u_1 = Q[a^2\mu^2 + b^2(1-\mu^2)]^{1/2} \quad (25)$$

$$u_2 = Q[(a+t_a)^2\mu^2 + (b+t_b)^2(1-\mu^2)]^{1/2} \quad (26)$$

$$j_1(x) = (\sin x - x \cos x)/x^2 \quad (27)$$

$$v_1 = \frac{4}{3}\pi ab^2 \quad (28)$$

$$v_2 = \frac{4}{3}\pi[(a+t_a)(b+t_b)^2 - ab^2] \quad (29)$$

Here, W_1 and W_2 have been defined by eq 16 and 18. Figure 5

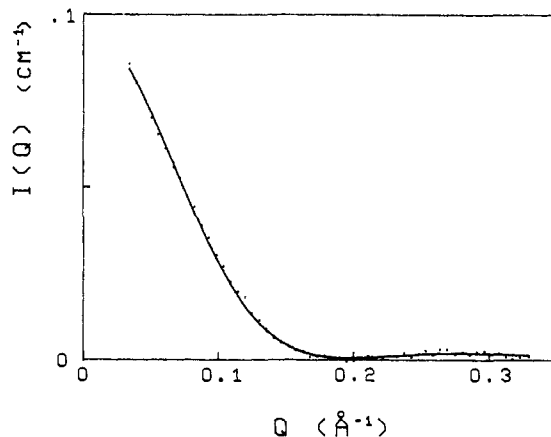


Figure 5. Scattering intensity profile for 0.049 M dihexanoyl-PC with perdeuterated fatty acyl chains in D_2O . The solid line is the profile computed from the proposed micellar structure, assuming $S'(Q) = 1$.

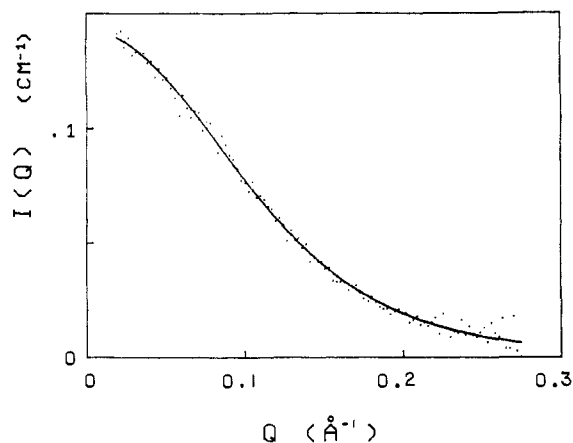


Figure 6. Scattering intensity profile for 0.050 M fatty acyl perdeuterated dihexanoyl-PC in H_2O . The solid line is the profile computed from the proposed micellar structure, assuming $S'(Q) = 1$.

shows the scattering intensities for the fatty acyl chain perdeuterated dihexanoyl-PC in D_2O , i.e., the case of $\alpha = 1$ and $\beta = 1$ in the external contrast variation. As mentioned previously, the scattering comes mostly from the head groups. The solid curve in Figure 5 is computed from eq 4 with $P(Q)$ given by eq 24 and I_0 obtained from the Guinier plot. The agreement between the model and the experimental data is good when one chooses $t_a = 6 \text{ \AA}$ and $t_b = 10 \text{ \AA}$. The fit becomes poor for the region $Q > 0.075 \text{ \AA}^{-1}$ when one chooses other sets of t_a and t_b , for example $t_a = t_b = 7.88 \text{ \AA}$ or $t_a = 4 \text{ \AA}$ and $t_b = 12 \text{ \AA}$, though these pairs of t_a and t_b do give the same value of $R_{g,2}$. Thus, the uncertainty of the values of t_a and t_b should be within about 10%. The profile of the neutron scattering spectrum is typical for the scattering from a shell-type object. A hump around $Q = 0.28 \text{ \AA}^{-1}$ is noticeable.

Since the mean csld of the head group is closer to ρ_{H_2O} than to ρ_{D_2O} , the scattering from the chain-perdeuterated dihexanoyl-PC in pure H_2O will have a higher contribution from the core than from the shell region. The weighting factor in terms of $W_1/(W_1 + W_2)$ is 0.745. Such a case can be used to test whether the hydrocarbon core is modeled properly. Figure 6 shows that the experimental data can be predicted by the proposed model very well. In order to fit the scattering intensities, the choice of $b = 7.83 \text{ \AA}$ is critical. The core volume given by $b = 7.83 \text{ \AA}$ and $a = 23.95 \text{ \AA}$ is just enough to contain the hydrocarbon tails of the dihexanoyl-PC micelle. Choosing a value of b less than 7.83 Å will result in a core volume smaller than what is necessary to contain the hydrocarbon tails. As an approximation, a single value of b greater than 7.83 Å can be used to represent the case when one of the semiminor axes of the micellar core is 7.83 Å and the other semiminor axis grows slightly larger than 7.83 Å. The result of choosing $b > 7.83 \text{ \AA}$ is that the core volume may be much larger than the volume of the hydrocarbon tails of a micelle. This is

(29) Cabane, B.; Duplessix, R.; Zemb, T. *J. Phys. (Les Ulis, Fr.)* in press.

(30) Franks, N. P. *J. Mol. Biol.* 1976, 100, 345.

(31) Buldt, G.; Gally, H. U.; Seelig, J.; Zaccari, G. *J. Mol. Biol.* 1979, 134, 673.

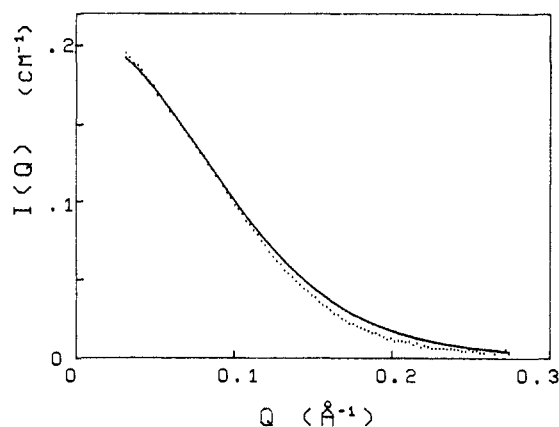


Figure 7. Scattering intensity profile for 0.027 M dihexanoyl-PC in D_2O . The solid line is the profile computed from the proposed micellar structure, assuming $S(Q) = 1$.

not possible unless one allows a large amount of water molecules to be present in the hydrocarbon core. None of the previous physical studies are consistent with such a model.^{5,10,23} Above all, noticeable errors in fitting the scattering intensities of Figure 6 appear if one uses a value of b that differs from 7.83 Å by about 5%.

To examine the possibilities of an oblate ellipsoidal structure, one can construct a model in a similar way by using the known values of $R_{g,1}$ and $R_{g,2}$. Considering that the hydrocarbon tails form a closely packed core, one will have $a = 4.4$ Å and $b = 18.4$ Å. A half-thickness of 4.4 Å is much smaller than the fully stretched tail length 7.83 Å, and also the core surface area is larger than that of a prolate ellipsoid. Taking a value of $a > 4.4$ Å will result in a core volume larger than the volume of the hydrocarbon tails of a micelle. In terms of fitting the scattering spectrum of Figure 6, these oblate ellipsoidal models could not fit the data as well as the prolate ellipsoidal model.

The third case to be presented is the scattering from proteo-dihexanoyl-PC in D_2O , i.e., $\alpha = 1$ and $\beta = 0$. From Table I, where the weighting factors are listed, one can see that the contributions from the head groups and from the core are both important. As shown in Figure 7, the agreement between the model and the experimental data is not as good as the two other cases, which were dominated by scattering from the head group and from the core, respectively. The agreement can be improved by choosing $t_a = 3$ Å or $t_b = 13$ Å or by allowing a small error of about 0.01 1/cm in subtracting the background.

Interactions between Micelles. When the concentration of micellar solutions is high and the volume fraction of the dihexanoyl-PC in the solution is more than a few percent, interactions between micelles can no longer be neglected. Incorporating the interaction between micelles in eq 4, we have

$$I(Q) = I_0 P(Q) S'(Q) \quad (30)$$

For a system consisting of monodispersed but nonspherical particles, the weighted interparticle structure factor $S'(Q)$ can be calculated approximately by assuming that the orientations of the particles are completely uncorrelated with their positions.³² One then has

$$S'(Q) = 1 + \beta(Q)[S(Q) - 1] \quad (31)$$

where

$$\beta(Q) = \frac{|\sum_{j=1}^N F_j(\vec{Q})|^2}{\sum_{j=1}^N |F_j(\vec{Q})|^2} \quad (32)$$

$$S(Q) = \frac{1}{N} \left(\sum_{j=1}^N \sum_{j'=1}^N \exp[i\vec{Q} \cdot (\vec{R}_j - \vec{R}_{j'})] \right) \quad (33)$$

Here, the vectors \vec{R}_j and $\vec{R}_{j'}$ in eq 33 are the position vectors of the center of mass of the particles. The function $\beta(Q)$ depends on the particle structure and has values varying between unity and zero. For the present micellar model, the function $\beta(Q)$ can be written explicitly as

$$\beta(Q) = \left| \int_0^1 \left[\left(w_1 - w_2 \frac{V_1}{V_2} \right) 3j_1(u_1) + \left(w_2 + w_2 \frac{V_1}{V_2} \right) 3j_1(u_2) \right] d\mu \right|^2 / \left\{ \int_0^1 \left[\left(w_1 - w_2 \frac{V_1}{V_2} \right) 3j_1(u_1) + \left(w_2 + w_2 \frac{V_1}{V_2} \right) 3j_1(u_2) \right]^2 d\mu \right\} \quad (34)$$

When a mean spherical approximation (MSA) is used, which relates the interparticle structure factor to the interparticle potential function, the $S(Q)$ in eq 33 can be obtained by solving the Ornstein-Zernike equation.³³ Although it is possible to solve for the multicomponent interparticle structure factors for a system consisting of spherical particles of different sizes interacting with each other through the corresponding hard cores plus Yukawa tails,³⁴ it is not possible for a system consisting of nonspherical particles like the dihexanoyl-PC micelles. Our approach is to calculate $S(Q)$ as though the particles are spherical and to take into account the effects of nonsphericity through the function $\beta(Q)$. This approach has been used successfully for studying the interactions between lithium dodecyl sulfate micelles³⁵ or between globular proteins.^{32,36}

A potential with a hard core plus a Yukawa tail has been widely used to model the interactions between colloidal particles. The potential function $U(r)$ is characterized by three parameters, the effective diameter σ , the dimensionless screening constant k , and the depth of the Yukawa tail γ (in unit of $k_B T$), and is given in a dimensionless form as

$$U(r)/k_B T = \begin{cases} \gamma \frac{e^{-k(x-1)}}{x} & x \geq 1 \\ \infty & x < 1 \end{cases} \quad (35)$$

Here, $x = r/\sigma$ and $k = \kappa\sigma$ where κ^{-1} is the decay length of the potential. Note that γ is negative for an attractive interaction. This kind of potential function may not be an entirely realistic description of the attractive interactions between micelles, but it certainly has the features that allow one to investigate the range as well as the strength of the interaction and also has the advantage of yielding an analytic solution of $S(Q)$ ³⁷ that is vital for fitting the experimental data. In the same way, Hayter and Zulauf³⁸ modeled the attractive force between the nonionic micelles formed by *n*-octylpentaoxyethylene glycol monoether in aqueous solutions near the lower consolute temperature. At high salt concentrations the intermicellar pair potential of lithium dodecyl sulfate micelles was found to be attractive and could be modeled by this form of potential as well.³⁵ In both cases the decay length of the potential was chosen to be about the van der Waals diameter of a water molecule, 2.9 Å.³⁹ In our analysis we determined k as well as γ and σ from fitting the experimental data to the theory.

Besides the three parameters mentioned above, $S(Q)$ also depends on another parameter, ϕ , the volume fraction of the micelles

(33) Ornstein, L. S.; Zernike, F. *Proc. Acad. Sci. (Amsterdam)* **1914**, *17*, 793.

(34) Blum, L.; Høye, J. S. *J. Stat. Phys.* **1978**, *19*, 317.

(35) Bendedouch, D.; Chen, S.-H.; Koehler, W. C. *J. Phys. Chem.* **1983**, *87*, 2621.

(36) Bendedouch, D.; Chen, S.-H. *J. Phys. Chem.* **1984**, *88*, 648.

(37) Cummings, P. T.; Smith, E. R. *Mol. Phys.* **1979**, *38*, 997.

(38) Hayter, J. B.; Zulauf, M. *Colloid. Polym. Sci.* **1982**, *260*, 1023.

(39) Krynicki, K.; Green, C. D.; Sawer, D. W. *Faraday Discuss. Chem. Soc.* **1978**, *66*, 199.

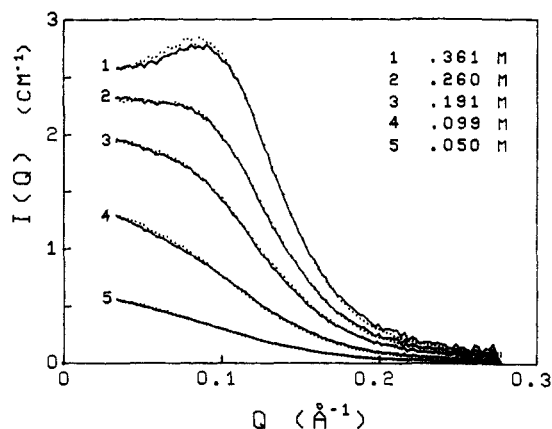


Figure 8. Scattering intensity profiles for different concentrations of dihexanoyl-PC in D_2O . The solid lines are the fitted curves, assuming the same particle form factor as that at 0.027 M lecithin. The parameters that characterize the interactions between the micelles are then determined from the fitting.

Table II. Parameters Derived from an Analysis of the Intermicellar Interactions of High Concentrations of Dihexanoyl-PC in D_2O

concn, M	ϕ	I_0, cm^{-1}	γ	k	$\sigma, \text{\AA}$
0.361	0.14	5.59	-1.74	14	51
0.260	0.099	4.09	-1.50	14	51
0.191	0.071	2.97	-1.45	14	51
0.099	0.034	1.58	-1.97	14	51
0.050	0.014	0.62	-2.64	14	51

in the solution, which represents the excluded volume effect. The parameter ϕ can be estimated by counting the total volume fraction occupied by the dihexanoyl-PC molecules in the micellar state. Thus, it is given by

$$\phi = V_m(C - C_{\text{cmc}}) \quad (36)$$

From fitting the experimental data according to eq 30, we find that the micellar structure does not change with concentration in the studied range of 0.027–0.361 M. Thus, the normalized micellar structure factor $P(Q)$ in eq 30 is assumed to be the same as that of the scattering spectra from a dilute solution of 0.027 M, at which $S'(Q)$ is essentially unity. I_0 , k , γ , and σ are obtained from the following fitting: σ is equal to 51 Å independent of the concentration; k is in the range of 12–16 to have the same goodness of fits. The average value of $k = 14$ was used in the final fitting of all the concentrations so that γ can be compared on the same ground.

Figure 8 shows the neutron scattering spectra from solutions containing 0.05–0.361 M dihexanoyl-PC in D_2O together with the fitted curves. The experimental data agree well with the micelle-micelle interaction model given in eq 30. The fitted parameters along with the computed ϕ are listed in Table II. The depression in the low- Q region is due to the increasing excluded volume effect as the micellar concentration is increased. This can be clearly seen in Figure 9 where $S'(Q)$ extracted from the scattering spectra is plotted for each concentration. One can see that the first diffraction peak occurs at about $Q = 0.123 \text{ \AA}^{-1}$. The first diffraction peak should occur at about $Q = 2\pi/\sigma$ for an intermicellar potential of the form given by eq 35. Thus, the value of σ should be about $2\pi/0.123 \text{ \AA}^{-1} = 51 \text{ \AA}$. From Table II we see that the fitted σ is equal to 51 Å. Theoretically, the value of σ can be understood by considering the structure of the micelle. When two micelles come close to each other, their approach is hindered by the water molecules hydrating the hydrophilic head groups. σ can thus be estimated by adding the thickness of the hydration shell (i.e., 2 times the diameter of a water molecule 5.8 Å) to the diameter of an equivalent sphere of the same volume as the two-region micelle (i.e., 42.4 Å) and multiplying by a correction factor of 1.04 for a spheroid having a major to minor axis ratio of about 1.6. The correction factor is determined by calculating the second virial coefficient by the method given by

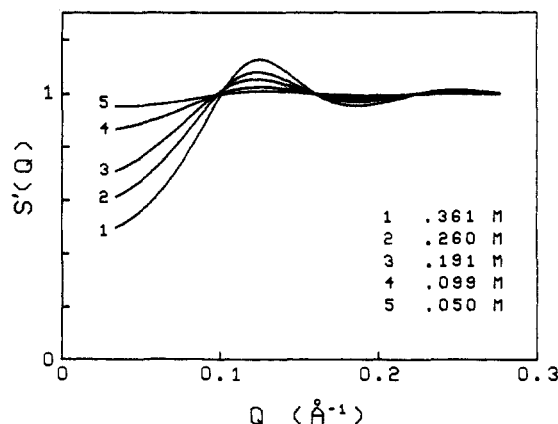


Figure 9. Interparticle structure factors corresponding to the cases shown in Figure 8, computed from the fitted parameters listed in Table II. The depression in the lower Q region and the buildup in the first peak become progressively pronounced as the concentration increases.

Ishihara and then equating it to the second virial coefficient of an equivalent hard sphere.³² This calculation gives $\sigma = 50.3 \text{ \AA}$, in good agreement with the result predicted by the model. If one tries to compute the total excluded volume fraction by assuming a rigid sphere of diameter about 51 Å, which is a correct procedure for a system of close-packed spherical micelles but may not be applicable for other situations, one will find that the experimental data cannot be fitted with such high values of ϕ .

In order to fit the scattering spectra, it is necessary to have $\sigma = 51 \text{ \AA}$ and a volume fraction ϕ given by considering only the volume fraction of the dihexanoyl-PC molecules that form micelles. Slight changes in the values of ϕ from the values shown in Table II as given by eq 36 do not hurt the fitting much, but the range of ϕ is well limited. Having the same n_p and ϕ , a system will have a hard-core diameter of 29 Å, which represents the unpenetrable part of the particle. In modeling the interaction potential, a Yukawa form is used. The model states that the attractive interaction starts at a center to center distance of σ in an averaged sense since the micelles are not spherical and decreases as the distance increases. In this way the potential model neglects the possibility of partial penetrabilities between the distances of σ and 29 Å. Instead, this potential model approximately preserves the right position of the most probable distance of closest approach of two micelles, if one reconciles the position of the maximum attraction point in the potential function, i.e., σ , with the smallest distance that two micelles can have between one another without any hindrance. This is expected to be about 50.3 Å as explained previously. Thus, the parameter σ should not be considered as the hard-core diameter that can be related to the excluded volume effect. The shell region of the micelle is partially penetrable since the head groups are flexible and the water molecules that constitute about 80% of the shell region in volume are relatively free to move. The true accessible volume to the micelles will be about the volume occupied by the dihexanoyl-PC molecules that form micelles. Thus, using eq 36 to calculate ϕ should be appropriate.

It is noted that $S'(Q)$ in the region $Q > 0.15 \text{ \AA}^{-1}$ is nearly unity for all cases. Plotting $I(Q)/I_0$ vs. Q should give similar profiles for different concentrations in the region $Q > 0.15 \text{ \AA}^{-1}$. Indeed, Figure 10 shows that the scattering spectra scaled by I_0 coincide in the tail region where only $P(Q)$ is important in determining the profile. This is direct evidence that the micelles do not grow with concentration at least up to a concentration of 0.361 M. The differences between the curves in Figure 10 are due solely to $S'(Q)$. As a check of consistency, the scattering amplitude I_0 is plotted as a function of concentration C and is shown in Figure 11. I_0 is found to be a linear function of C , which means that the aggregation number does not change with concentration. The slope of the straight line is extrapolated to cross the zero intensity line at the critical micellar concentration.

The interaction between micelles is modeled by an effective interparticle pair potential or the so-called potential of mean force by treating the solvent as a structureless continuum. The situation

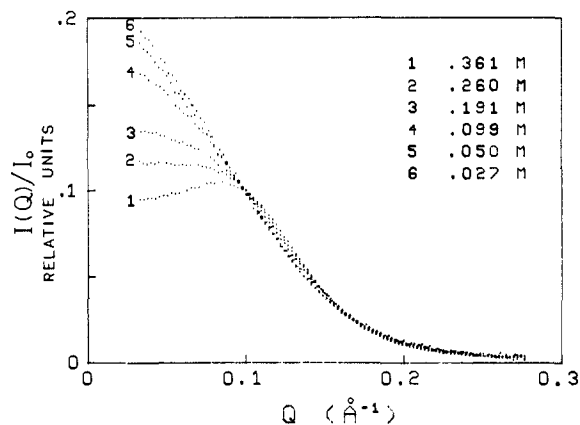


Figure 10. Scattering intensity profiles scaled by their scattering amplitudes to show how the product $P(Q)S'(Q)$ changes with the concentration. These curves are seen to coincide very well for $Q > 0.15 \text{ \AA}^{-1}$, implying that the particle size and the structure do not change with the concentration.

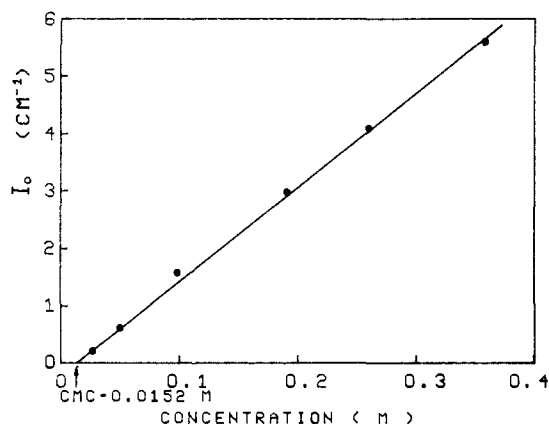


Figure 11. Scattering amplitudes determined from the fitting plotted vs. the lecithin concentration to yield a straight line that gives the critical micellar concentration as 0.0152 M and an aggregation number of 19.

is different from a true one-component system, for example, the argon gas. The micelles are in fact immersed in the solvent, and the solvent molecules have a finite size and their own structure. Effects due to the existence of solvent molecules are not explicitly taken into account but may be reflected in the parameters like the decay length and strength of the interaction. From values of $\sigma = 51 \text{ \AA}$ and $k = 14$ we have the decay length of the potential $\kappa^{-1} = 3.64 \text{ \AA}$. This value is close to the value used by Hayter and Zulauf³⁸ from consideration of the effects of structured water surrounding a nonionic micelle. The study of phase separation of nonionic surfactants in aqueous solutions by Kjellander⁴⁰ surrounding that the range of the force compared with the size of the micelle should be small. The result of this study supports these ideas.

The values of γ vary from -1.45 to -1.97 for concentrations from 0.088 to 0.361 M. For low-concentration cases the interaction is weak; thus, it is more difficult to determine γ accurately from the fitting. The interaction is clearly an attractive one. The origin of the attraction must be of the van der Waals type including the dispersion forces and dipole-dipole interactions. But, the effective pair potential between micelles should include considerations such as the finite size of water molecules and the ordering of the water molecules near the micellar surfaces. This could be the reason why we did not find the same γ for all concentrations as it should be for a true one-component system. An attractive potential of a few $k_B T$ is quite reasonable for the generally accepted values of Hamaker constants.⁴¹

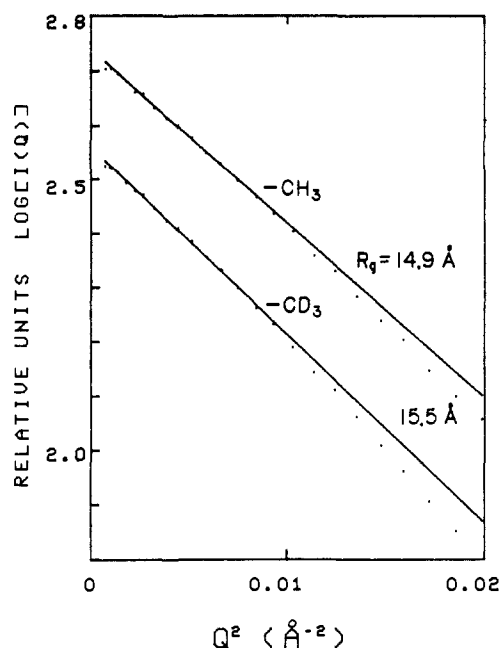


Figure 12. Guinier plots of the di(hexanoyl- $6,6,6-d_3$)-PC and the proteo compound in D_2O solvent. The radii of gyration of both cases are shown.

Distribution of Methyl Groups. The ordering and conformation of the fatty acyl chains in the core region is important for understanding micelle structure. In particular, an analysis of the distribution of the terminal methyl groups can provide evidence for or against the NMR and Raman view of the lecithin chains as highly disordered.⁵ The mean csld of the methyl group is very close to the mean csld of the tails. Thus, we deuterated only the terminal methyl groups and compared the neutron scattering spectra for this species with the proteo compound at the same concentration (0.050 M in D_2O). If the micellar structure is spherically symmetric, it is possible to obtain the distribution of the end groups in Q space by taking the difference between the square route of the scattering intensities from the terminal methyl deuterated and the proteo species at the same dilute concentration.¹⁹ For dihexanoyl-PC micelles the averaging over orientations of the nonspherical micelles makes it impossible to carry out the same analysis procedure. Instead, we have determined the radius of gyration from Guinier plots as shown in Figure 12. The radius of gyration of the CD_3 -containing micelle is 15.5 \AA , which is larger than the value of 14.9 \AA for the proteodihexanoyl-PC micelles. This is expected since deuteration reduces the contrast of the core region.

The contributions of the dihexanoyl-PC molecule to the radius of gyration of the micelle can be divided into two parts. The first part is from the terminal methyl group, which depends on whether it is deuterated or not. The second part is from the rest of the molecule, which remains the same. Similar to eq 14 but with subscripts 1 and 2 now representing the end group and the rest of the molecule, we can solve for R_{g1} and R_{g2} using the two known R_g 's for the methyl deuterated and the proteolecithins. The volume of each methyl group is assumed to be equal to 54.3 \AA^3 in the calculation of W_1 and W_2 . The result is that the terminal methyls have a radius of gyration of 11.36 \AA . If the end groups are distributed uniformly within the hydrocarbon core, the radius of gyration should be equal to that of the core, i.e., 11.8 \AA . If the end groups are packed close to the center of the core, they will form a spheroidal region with a major axis of 20.95 \AA and a minor axis of 4.83 \AA in order to accommodate all the end groups; this leaves a surface layer 3 \AA in thickness for the other part of the tails. The terminal methyl groups will have a radius of gyration of only 9.85 \AA . A value of 11.36 \AA indicates that the actual situation is closer to a uniform distribution with higher probabilities in the center region than on the surface. In order to have a radius of gyration of 11.36 \AA , the end groups in the center region must be 1.8 times the probability in the 3- \AA -thick surface layer, which

(40) Kjellander, R. *J. Chem. Soc., Faraday Trans. 1* 1982, 78, 2025.

(41) Ohshima, H.; Inoko, Y.; Mitsui, T. *J. Colloid Interface Sci.* 1982, 86, 57.

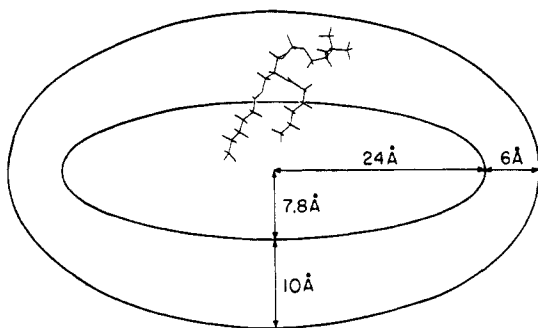


Figure 13. Model for dihexanoyl-PC micelles based on SANS contrast variation results. The orientation of the dihexanoyl-PC is based on truncating the chains of crystal structures of dilauryl-PC and dimyristoyl-PC (i.e., all *trans* chains tilted with respect to the surface normal). The glycerol backbone and carbonyls are not included in the hydrocarbon core.

means that about half of the terminal methyls are in the surface layer. This is in contrast to the more ordered behavior (as monitored by neutron diffraction) of terminal methyl groups in dipalmitoyl-PC bilayers in the liq. cryst. phase.⁴² A degree of ordering of the hydrocarbon chain in the core region does exist, but certainly the terminal methyls are not packed closely in the center of the hydrocarbon core.

Conclusions

The SANS results of the structure of dihexanoyl-PC micelles can be summarized in the following five main points:

1. The micellar structure of this short-chain lecithin can be well represented by a prolate ellipsoid with two uniform regions. From the radii of gyration from external and internal contrast variation measurements, we have determined uniquely the radii of gyration for the two regions: the region consisting of the fatty acyl chains has a radius of gyration of 11.8 ± 0.2 Å, and the region containing the hydrophilic head groups has a radius of gyration of 18.4 ± 0.3 Å.

2. The hydrocarbon tails for a close-packed core of a spheroidal shape have a minor axis equal to the fully stretched tail length 7.83 Å and a major axis equal to 23.95 Å. The head groups are distributed in a shell region surrounding the hydrocarbon core with a shell thickness of 10 Å in the direction of the minor axis and 6 Å in the direction of a major axis. This structural model satisfactorily predicts the entire Q dependence of the SANS spectra at various contrast conditions. The space between the

(42) Zaccai, G.; Buldt, G.; Seelig, A.; Seelig, J. *J. Mol. Biol.* 1979, 134, 693.

hydrophilic head groups is considerably larger in a micelle structure (102 Å² per head group) than in a monolayer structure (65 Å² per head group⁴). This may in part explain why these micelle aggregates are much better substrates for phospholipases than lecithin bilayers. With the larger area per head group, the phospholipase presumably has better access to the substrate. The thickness of the hydrophilic shell region implies that the head group must have an orientation parallel to the surface of the hydrocarbon core. This model for the dihexanoyl-PC molecule is schematically shown in Figure 13.

3. Dihexanoyl-PC micelles were found to be monodispersed in the whole concentration range studied. The aggregation number remains at 19 ± 1 throughout the range from 0.027 to 0.361 M. We have confirmed that dihexanoyl-PC micelles do not grow with increasing concentrations,⁴ in contrast to most micelles.²⁸

4. The interaction between dihexanoyl-PC micelles was found to be attractive at all concentrations. It can be modeled successfully by an effective potential of the form of a hard core plus an attractive Yukawa tail. The parameters characterizing the interaction were determined from fitting the SANS spectra at different concentrations with the micellar interaction model. A constant effective core diameter of 51 Å was found that could be explained well by considering the micellar structure together with the effect of a hydration layer. The strength of the attraction turns out to be between 1 and 2 $k_B T$, which is comparable to the magnitude of the Hamaker constant. The decay length of the attraction is about 3.64 Å, which is of the order of the size of the solvent molecule. This result suggests that the structure of the solvent around the interface may be important in determining the effective interaction between micelles.

5. The distribution of the fatty acyl chain terminal methyl groups in the hydrophobic core was studied by comparing the radius of gyration of the di(hexanoyl-*6,6,6-d*₃)-PC to that of proteodihexanoyl-PC micelle. There is no preferential ordering near the center of the micelle. Instead, the terminal methyls are distributed in the whole core with a slightly higher probability toward the center. Such a highly disordered structure is, in fact, consistent with spectroscopic studies of these micelles.

Acknowledgment. We are grateful to the Biology Department of Brookhaven National Laboratory and to the National Center for Small Angle Scattering Research for the use of their respective spectrometers in this work. This research is supported by the Petroleum Research Fund, administered by the American Chemical Society (S.-H.C.), and NIH Grant GM26762 (M.F.R.). T.-L.L. acknowledges financial support of a T. J. Thompson Fellowship from the Nuclear Engineering Department, MIT.

Registry No. I, 34506-67-7; neutron, 12586-31-1.

Communications to the Editor

On the Stability of the PdH₂ Molecule

C. Jarque and O. Novaro

*Instituto de Fisica, U.N.A.M.
Apdo. Postal 20-364, Mexico 01000 D.F.*

M. E. Ruiz* and J. Garcia-Prieto

*Instituto Mexicano del Petróleo
Apdo. Postal 14-805, Mexico 07730 D.F.*

Received June 5, 1985

The Pd($4d^{10}5s^0$, 1S) + H₂($^1\Sigma_g^+$) \rightleftharpoons PdH₂ reaction has been studied for the C_{2v} symmetry by several authors.¹⁻³ They agree

that a weakly bound $^1A_1(C_{2v})$ palladium dihydride if formed without any appreciable activation barrier for this side-on approach of H₂ on the ground state Pd atom. No theoretical studies exist, to our best knowledge, for the alternative head-on approach of H₂ on the same Pd state that could in principle lead to a Pd-H-H dihydride where the H atom moieties would *not* be equivalent for the IR absorption bands of this complex, as would be the case of the side-on complex.

(1) Brandemark, U. B.; Blomberg, M. R. A.; Peterson, L. G. M.; Siegbahn, P. E. M. *J. Phys. Chem.* 1984, 88, 4617.

(2) Low, J.; Goddard, W. A., III. *J. Am. Chem. Soc.* 1984, 106, 8321.

(3) Yonezawa, T.; Nakatsuji, H.; Hada, M.; International Congress on Quantum Chemistry, Montreal, Canada, July 1985; Paper 24-A.